Interannual cycles of Hantaan virus outbreaks at the human–animal interface in Central China are controlled by temperature and rainfall

Huaiyu Tian[a,1], Pengbo Yu[b,1], Bernard Cazelles[c,d], Lei Xu[e,f], Hua Tan[g], Jing Yang[a], Shanqian Huang[a], Bo Xu[h], Jun Cai[h], Chaofeng Ma[i], Jing Wei[b], Shen Li[b], Jianhui Qu[j], Marko Laine[k], Jingjun Wang[b,2], Shilu Tong[l,m,n], Nils Chr. Stenseth[f,2], and Bing Xu[a,h,2]

[a]State Key Laboratory of Remote Sensing Science, College of Global Change and Earth System Science, Beijing Normal University, Beijing 100875, China; [b]Shaanxi Provincial Centre for Disease Control and Prevention, Xi'an 710054, Shaanxi, China; [c]Institut de Biologie de l'École Normale Supérieure UMR 8197, Eco-Evolutionary Mathematics, École Normale Supérieure, 75230 Paris Cedex 05, France; [d]Unité Mixte Internationnale 209, Mathematical and Computational Modeling of Complex Systems, Institut de Recherche pour le Développement et Université Pierre et Marie Curie, 93142 Bondy, France; [e]State Key Laboratory of Infectious Disease Prevention and Control, National Institute for Communicable Disease Control and Prevention, Chinese Center for Disease Control and Prevention, Beijing 102206, China; [f]Centre for Ecological and Evolutionary Synthesis, Department of Biosciences, University of Oslo, N-0316 Oslo, Norway; [g]Center for Bioinformatics and Systems Biology, Department of Radiology, Wake Forest School of Medicine, Winston-Salem, NC 27157; [h]Ministry of Education Key Laboratory for Earth System Modelling, Department of Earth System Science, Tsinghua University, Beijing 100084, China; [i]Xi'an Centre for Disease Control and Prevention, Xi'an 710054, Shaanxi, China; [j]Hu County Centre for Disease Control and Prevention, Xi'an, Shaanxi 710302, China; [k]Finnish Meteorological Institute, Helsinki FI-00101, Finland; [l]Shanghai Children's Medical Center, Shanghai Jiao Tong University, Shanghai 200127, China; [m]School of Public Health and Institute of Environment and Population Health, Anhui Medical University, Hefei 230032, China; and [n]School of Public Health and Social Work, Queensland University of Technology, Kelvin Grove, QLD 4059, Australia

Edited by Burton H. Singer, University of Florida, Gainesville, FL, and approved June 13, 2017 (received for review February 1, 2017)

Hantavirus, a rodent-borne zoonotic pathogen, has a global distribution with 200,000 human infections diagnosed annually. In recent decades, repeated outbreaks of hantavirus infections have been reported in Eurasia and America. These outbreaks have led to public concern and an interest in understanding the underlying biological mechanisms. Here, we propose a climate–animal–Hantaan virus (HTNV) infection model to address this issue, using a unique dataset spanning a 54-y period (1960–2013). This dataset comes from Central China, a focal point for natural HTNV infection, and includes both field surveillance and an epidemiological record. We reveal that the 8-y cycle of HTNV outbreaks is driven by the confluence of the cyclic dynamics of striped field mouse (*Apodemus agrarius*) populations and climate variability, at both seasonal and interannual cycles. Two climatic variables play key roles in the ecology of the HTNV system: temperature and rainfall. These variables account for the dynamics in the host reservoir system and markedly affect both the rate of transmission and the potential risk of outbreaks. Our results suggest that outbreaks of HTNV infection occur only when climatic conditions are favorable for both rodent population growth and virus transmission. These findings improve our understanding of how climate drives the periodic reemergence of zoonotic disease outbreaks over long timescales.

Hantaan virus | spillover to humans | wildlife reservoir | time-series data | climate change

The seasonality and dynamic patterns of many infectious diseases have attracted substantial research interest for a long time, especially in the case of zoonotic diseases (1–3). Outbreaks are driven by many factors, such as environmental conditions, a decrease in the immunity levels within the host population, increasing natural population densities of the wildlife reservoir, and an increase in reservoir–human interactions (4). Most previous studies have focused on the seasonal variation of infectious diseases. However, studies concerning the interannual variability of zoonotic epidemics have been limited and highly controversial, chiefly because of the scarcity of long-term records on both human disease cases and animal surveillance, and difficulties quantifying the role of environmental forcing in animal–human transmission systems. Here, we combine animal surveillance data with epidemiological records of hemorrhagic fever with renal syndrome (HFRS) for the past one-half century in the Weihe Plain, a natural Hantaan virus (HTNV) infection focal point in Central China (Fig. 1) (5). We examine whether the observed interannual cycles were driven by external factors, such as climate and/or animal population dynamics.

Hantaviruses (genus *Hantavirus*, family *Bunyaviridae*) are negative-sense single-stranded RNA viruses (6) that can cause serious diseases in humans, and in certain outbreaks can lead to mortality rates of 12% (HFRS) and 60% (hantavirus pulmonary syndrome) (7). Collectively, hantaviruses account for an estimated 200,000 clinical cases of disease annually on a global basis (8). In mainland China, HFRS remains an important public health issue because >1.5 million HFRS cases were reported in this region alone during 1950–2010 (9). Human infection with hantaviruses occurs through exposure to aerosolized rodent excreta containing the pathogenic virus, when the environment for transmission is suitable (10, 11). In contrast, infection between rodents mainly results from aggressive encounters and biting (12, 13). Previously, it has been suggested that a link exists between

Significance

Interannual cycles of many zoonotic diseases are considered to be driven by climate variability. However, the role of climate forcing in the modulation of zoonotic dynamics has been highly controversial, chiefly due to the difficulty in quantifying the links between climate forcing, animal population dynamics, and disease dynamics. Here, we address this issue by using a unique field surveillance dataset from Central China, covering one-half century. Our results shed light on the drivers behind interannual variability and the dynamic patterns of disease ecology, and the links between interannual climate variability and the human–animal interface, adding up to 3-mo lead time over outbreak warnings.

Author contributions: H. Tian, J. Wang, N.C.S., and Bing Xu designed research; H. Tian, P.Y., C.M., J. Wei, S.L., J.Q., J. Wang, N.C.S., and Bing Xu performed research; P.Y., B.C., and H. Tan contributed new reagents/analytic tools; H. Tian, L.X., J.Y., S.H., Bo Xu, J.C., and M.L. analyzed data; and H. Tian, B.C., S.T., and N.C.S. wrote the paper.

The authors declare no conflict of interest.

This article is a PNAS Direct Submission.

Freely available online through the PNAS open access option.

[1]H. Tian and P.Y. contributed equally to this work.

[2]To whom correspondence may be addressed. Email: n.c.stenseth@ibv.uio.no, jingjunwang@china.com, or bingxu@tsinghua.edu.cn.

This article contains supporting information online at www.pnas.org/lookup/suppl/doi:10.1073/pnas.1701777114/-/DCSupplemental.

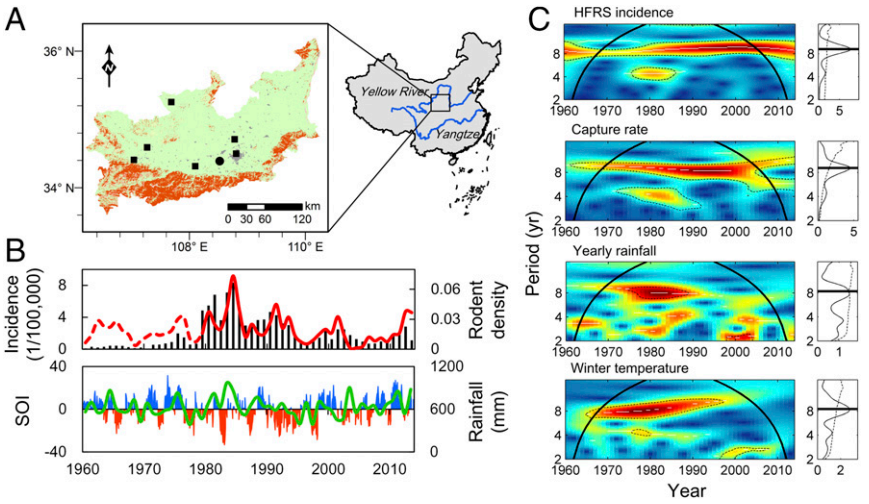

Fig. 1. Time series of climatic, surveillance, and epidemiological data. (*A*) Map of the Weihe Plain in Central China (106–110 °E, 34–36 °N), showing the weather station (rectangles) and sampling sites (circle; Hu County), croplands (green), artificial surfaces (gray), and areas overlapping the massif (orange). Since 1980, field surveillance of rodent dynamics has been carried out monthly. (*B*) The annual time series of HFRS incidence (bars) between 1960 and 2013, *A. agrarius* population density (red line), and the reconstructed population (*Materials and Methods*) density (dashed line) as provided by the optimal model. Rainfall (green line) and the Nino3.4 index, which serves as a proxy for ENSO (blue bars represent La Niña and red bars represent El Niño), are also shown. (*C*) Wavelet power spectra of the annual time series showing the periodicity of the incidence of HFRS, capture rate of striped field mouse, rainfall, and winter temperature. Wavelet power spectra are depicted in *C*, *Left*, and global wavelet power spectra are in *C*, *Right*. In the wavelet power spectra, the dotted line corresponds to the 5% significance level, and the bold line is known as the cone of influence. This line delimits the effect of the treatment of the boundaries. The white lines materialize the maxima of the undulations of the wavelet power spectra, and the colors code for power values from blue (low values) to red (high values). *C*, *Right* shows the mean spectrum (vertical solid black line) with its significant threshold value of 5% (dashed line).

outbreaks of hantavirus infection, the population dynamics of the carrier rodents, and climate variability (14–16) in Asia (16–19), Europe (20), and the Americas (21–24). However, outbreaks of zoonotic hantaviruses do not simply track environmental conditions or rodent dynamics (25, 26). A critical knowledge gap still remains between key environmental drivers, population dynamics of animal reservoirs, and human infections that account for the ecology and epidemiology of hantaviruses. The mechanisms that underscore the interannual variability of the transmission dynamics of hantaviruses at the animal–human interface are poorly understood as well.

The overall aim of this study was to determine the role climate forcing plays in the observed human–animal–HTNV dynamics, spanning 54 y, through model fitting and simulation. Additionally, the study aimed to evaluate the effect of climate forcing on both the population change in the wildlife reservoir and the fluctuations in HFRS outbreaks on both seasonal and interannual timescales. We investigated the dynamics of HFRS epidemics through the following three components: rodent population density, human incidence of disease, and climate variability.

Results

There Is an 8-y Confluence of HFRS, Reservoir, and Climatic Conditions. Concurrent changes between climate (especially amount of rainfall) and the incidence of disease within the animal reservoir and human population were observed over a long period in the Weihe Plain of Central China (Fig. 1 *A* and *B*). A strong positive correlation was observed between the annual incidence of HFRS and the capture rate of *Apodemus agrarius* ($R = 0.77$, $P < 0.01$) and between the capture rate of *A. agrarius* and rainfall in the last year ($R = 0.40$, $P < 0.01$). Wavelet analyses confirmed that all of the time series studied in the Weihe Plain—including the number of HFRS cases, capture rate of rodents, amount of annual rainfall, and average winter temperature—showed interannual oscillations of 8- to 10-y dominant periods between the 1960s and 2010s (Fig. 1*C*). The resulting periodicities seem likely to occur from the superimposition of the El Niño–Southern Oscillation (ENSO), which strongly affects local climate. It is worth noting that only winter temperature showed an 8-y periodicity, whereas spring, summer, autumn, and annual mean temperatures did not (*SI Appendix*, Fig. S1). These findings suggest that the interannual variation in the HFRS epidemics over long timescales may be related to rodent population dynamics and climate variability.

Here, we report the interannual variability of climate, animal reservoir, and HFRS outbreaks. Significant relationships were found between these variables, and the potential impact of ENSO on the 8-y pattern of epidemics was highlighted.

Reservoir Dynamics Are Associated with Climatic Conditions in Linear and Nonlinear Ways. The optimal rodent model fitted with the generalized additive model (GAM) framework that best reflected the population dynamics from 1980 to 2013 (Fig. 2*A*; $R = 0.81$, $P < 0.01$) was used to reconstruct the dynamics during 1960–1979. The results showed the positive feedback of *A. agrarius* abundance (Fig. 2*B*), nonlinear positive effects of amount of annual rainfall (Fig. 2*C*), and an intriguing nonlinear relationship between winter temperature and the capture rate of *A. agrarius* (Fig. 2*D*). The M-shaped curve revealed that extremely high/low winter temperatures (>1 °C or below −1.5 °C) may significantly reduce the population growth rate, thereby negatively affecting rodent abundance. The pivotal point occurred at approximately −0.5 °C, because a strong negative correlation between temperature and rodent abundance was found at approximately −1.5 and −0.5 °C, whereas a strong positive correlation between temperature and rodent abundance was found at approximately −0.5 and 1 °C. Our results indicate that when climatic conditions were incorporated into models of rodent population dynamics, winter temperature had strong effects on the overwinter abundance trajectory. Winter temperature, in combination with the previous year's rodent density and amount of rainfall, explained the population dynamics in the following year.

Here, we show that population dynamics of *A. agrarius* may respond to climatic conditions, including rainfall (which affects food availability) and temperature (which affects winter survival),

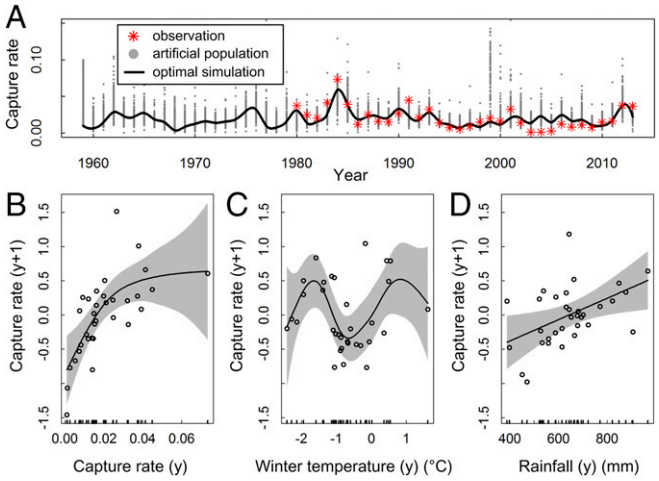

Fig. 2. The results of generalized additive models for *A. agrarius*. (*A*) Rodent population dynamics. Shown are 1,000 rodent population runs of the stochastic model in Eq. **1**; the gray points show all artificial populations simulated, the red points are the annually observed rodent populations, and the black line indicates the result of the optimal model (R = 0.81). (*B–D*) Partial effects of the annual density (*B*), last winter temperature (*C*), and rainfall (*D*). Shaded areas are 95% confidence bands. Winter temperature is calculated from December to January.

and infer the mode of how climate influences the interannual cycle of reservoir dynamics.

When HFRS Epidemics Occur, They Are Seasonal and Associated with Lagged Climatic Conditions. HFRS epidemics show strong seasonal dynamics. Although the magnitude of outbreaks varies greatly from year to year, the timing invariably coincides with the end of the rainy season in autumn (Fig. 3*A*). Our analysis focused on detecting seasonal changes in climate and evaluating whether climate variability is a determinant of fluctuations in HFRS epidemics. A strong negative correlation was observed between the incidence of HFRS and summer temperature ($R = -0.48$, $P < 0.01$). In contrast, the incidence of HFRS was positively correlated with summer rainfall levels ($R = 0.35$, $P < 0.01$) (Fig. 3 *B* and *C*; the randomization test is shown in *SI Appendix*, Fig. S2).

Here, we demonstrate that powerful seasonal forcing of HFRS transmission might be driven by specific environmental conditions or contact rates between humans and the reservoir host. Moreover, our results (*SI Appendix*, Fig. S3) clearly show that local climate is responsible for the statistically significant association between HFRS epidemics and environmental variables.

HFRS Is Causally Predicted by a Combination of Direct and Indirect Climatic and Reservoir Factors. The SEM analysis (Fig. 3*D* and *SI Appendix*, Table S1 and Fig. S4) consistently supported the previous analysis and indicated the following pathways: Rodent dynamics have a direct positive effect on HFRS epidemics; rainfall has an indirect positive effect via rodents; and temperature has a direct negative effect on HFRS epidemics. Based on these findings, we modeled HTNV spillover into human populations using monthly HFRS cases (the average R^2 train and R^2 test of cross validation are 0.93 and 0.85, respectively; *SI Appendix*, Fig. S5). The resulting model linking the rodent population system with the HFRS system is nonlinear, incorporating temperature and rainfall as environmental drivers (summarized in Fig. 4 and *SI Appendix*, Tables S2 and S3).

Concurrent changes in rodent population dynamics (Fig. 1*B*) provide evidence for the forcing of HTNV transmission by drivers at interannual timescales, and the additional effects of environmental forcing on the transmission rate are contained in the residuals. This finding allows us to quantify the role of environmental factors in the dynamics of HFRS. In Fig. 4, the magnitude of epidemic peaks is temporally aligned with the fraction of transmission rate. In times of high transmission, the incidence of HFRS would be expected to increase. However, the magnitude of the response is only high at a subset of these times. Most notably, the number of HFRS cases was low for 2002–2010, despite climatic conditions favorable toward a high transmission rate (Fig. 4*B*). This unexpectedly low response was concurrent with a low rodent density. These results emphasize that HFRS outbreaks occur only when climatic conditions are favorable for both rodent population growth and virus transmission.

Here, we interpret the mechanism of seasonal and interannual variability of HFRS incidence, resulting from a combination of direct and indirect climatic and reservoir factors (Figs. 1–3). Our findings also highlight that the nonlinear dynamics of climate forcing plays a role in seasonal transmission rates, but not when operating on interannual timescales (*SI Appendix*, Fig. S6).

Discussion

Zoonotic systems are shaped by complex interactions between the environment, wildlife cycle, and nonlinear spillover dynamics. The quality of the Weihe Plain dataset provides us with a unique opportunity to generate climate-driven models for zoonotic disease dynamics. We have provided a formal framework to understand the transmission dynamics of hantaviruses, which could account for the ecology of this zoonotic pathogen. Our study has shown the close link between interannual cycles of climate–animal–HFRS

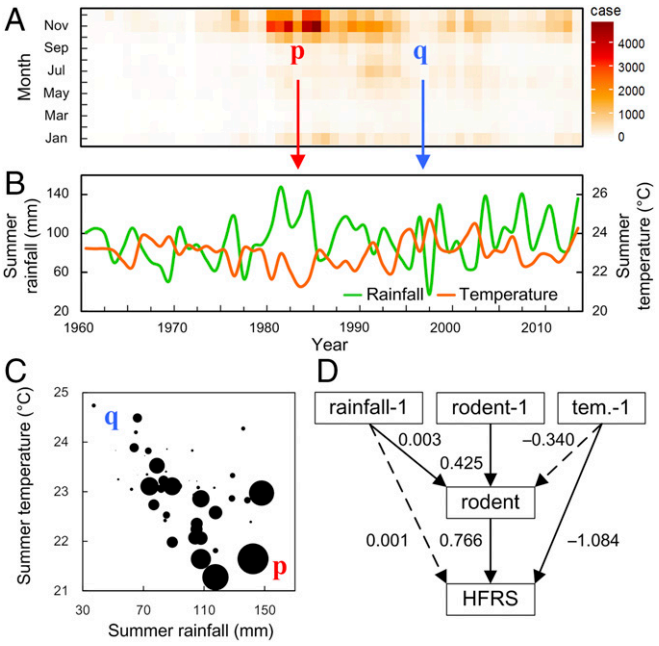

Fig. 3. Time series of monthly HFRS cases, summer rainfall, and the summer temperatures in the Weihe Plain, during the past 54 y. (*A*) Monthly distribution of HFRS cases. The number of HFRS cases (*x* axis, time in year; *y* axis, month in year) ranges from a low value (in white) to a high value (in dark red). (*B*) Summer rainfall (green line) and summer temperature (orange line). (*C*) Scatterplot of summer temperature (negatively associated with HFRS cases, $R = -0.48$, $P < 0.01$), summer rainfall (positively associated with HFRS cases, $R = 0.35$, $P < 0.01$), and HFRS cases (circle size is proportionate to the number of HFRS cases). p (red) and q (blue) represent zoonotic outbreaks and nonoutbreaks with corresponding summer climate conditions, respectively. Summer climate conditions are calculated from May to September. (*D*) Structure and results from our structural equation models for climate-linked HFRS epidemics. Values associated with arrows represent standardized path coefficients. The dashed lines represent nonsignificant paths; −1, previous year; rainfall, total annual rainfall; tem., mean annual temperature.

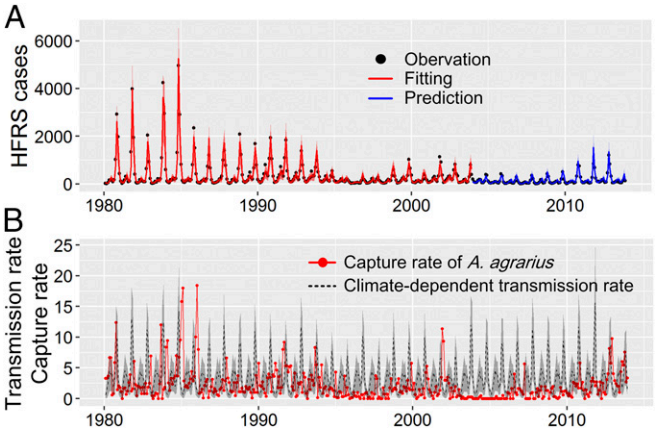

Fig. 4. Results of the nonlinear disease transmission model. (*A*) Temporal dynamics of observed vs. predicted HFRS cases. HFRS cases from rodent population models derived from data from 1980 to 2003. Observations are in black, fitted values are in red, and predictions for 2004–2013 are in blue. (*B*) The rodent population density and climate-dependent transmission rate; the corresponding shaded areas indicate the 95% credible intervals of the model fit.

outbreaks and reported on the climate-driven changes in reservoir dynamics and HFRS outbreaks. Finally, by bringing together these findings, we reveal the HTNV cycle in relation to key climate variables and the overlapping interannual, seasonal, and zoonotic cycles (Fig. 5).

Our study provides biological insight into the seasonality of spillover transmission, wherein hantaviruses transmit from animals to humans through seasonal animal–human contact rates (25), and the variation in encounters with environmental drivers. In addition, our study offers a window into the fundamental question of interannual variation in the dynamics of zoonotic hantaviruses. Here, we show how climate drives the cyclic pattern of HFRS outbreaks through the effect of both rainfall and temperature variations on wildlife life cycles and seasonal spillover dynamics. Understanding the timing and potential causes of epidemic cycles offers vital insights into how zoonotic system operate and highlights general insights into the climate drivers that influence the transmission of pathogens that are relevant to public health issues. This finding also emphasizes the potential risk of extrapolating dynamics for this zoonotic system without first fully considering and understanding the nonlinear nature of ecosystems.

The analysis reveals that large-scale wildlife reservoir dynamics are dominated by several interlinked factors (27, 28). The resulting high-amplitude rodent population interacts with climatic conditions and human activities to generate fluctuating epidemics of HFRS. Rainfall plays a role in HFRS dynamics and is positively linked with the risk of HTNV transmission. We assumed that high primary productivity resulting from high levels of precipitation could supply enough food for the growth of juvenile and subadult rodents (29). Thus, a high abundance of rodent hosts would amplify spillover through frequent contacts between rodents within the reservoir and human beings. It should be noted that the dynamics of zoonoses involve multiple phases (30). Through long-term field studies, an integrated picture (27) is revealed of the role that climate variability plays in the animal reservoir and infection risk to humans.

Temperature, the second climate variable of importance, is statistically correlated with rodent population growth and HTNV transmission rates. We have provided strong support for the hypothesis that winter temperature exerts complex effects on the rodent population growth rate (Fig. 2*C*). The relationship between winter temperature and rodent population growth rate varied between −1.5 and 1 °C, and we infer that these ranges are consistent with the temperature for snowmelt and formation of ice in winter. Freeze–thaw events are most likely to occur, which may affect food availability and the overwinter survival of rodents (31–33). Previous studies have shown that density-dependent effects on rodent growth can be altered by winter conditions (31). Increasing winter temperatures provide a survival benefit to increasing rodent populations. However, this increase might be associated with strong intraspecific competition due to food or space limitation (34, 35), resulting in a negative-feedback effect of density (Fig. 2*B*) (18, 31) and nonlinearity and nonmonotonic dynamics. The influence of density-dependent effect and winter temperature on rodent growth were supported by our results (Fig. 2 *B* and *C*). Concerning the negative impact of high summer temperature on the incidence of HFRS, the mechanistic link is not yet well documented. We hypothesize that high summer temperatures may constrain rodent activity or reduce the frequency of direct and indirect contact between infected donors and susceptible rodents or contact between rodents and human beings. Previous studies of rodent activity have shown that an increase in both ambient and soil temperatures was associated with a shortening of activity by earlier offsets of activity (36). Rodents are not able to maintain high body temperatures because this would result in heat prostration and eventual death. Instead, wild rodents deal with ambient increases in temperature by seeking shade or underground shelter (37). Additionally, high summer temperatures and a dry environment can reduce the survival rate of hantaviruses (38, 39). This reduction, in turn, could reduce potential infectious contact between rodents and eventually reduce the prevalence of HTNV.

Our results indicate the complex impact of climate change on important zoonoses, such as HFRS epidemics, due to both nonlinear and complex interactions between climate, pathogen, and host shape spillover dynamics. Global warming may affect rodent winter survival through winter temperatures by a complicated process, and it may also influence the magnitude of HFRS outbreaks through summer climatic conditions (both temperature and rainfall). Additionally, as global climate change accelerates, it will become more difficult to predict the estimated amount of annual rainfall accurately. In conclusion, climate change could lead to different patterns of hantavirus transmission and outbreaks among animals and human beings.

ENSO is considered to be a remote driver of interannual climate variability of local temperature and rainfall around the world and could influence the population dynamics of small mammals (40). Previous literature has shown an association between ENSO

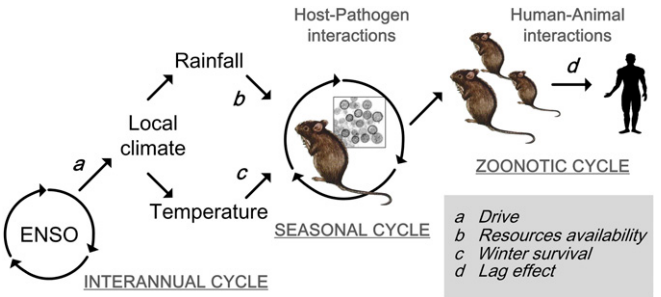

Fig. 5. Schematic of the HTNV cycle in the host *A. agrarius*, depicting climate variables as drivers. The model formulation is given in *Materials and Methods*. The solid line indicates available data, used in models linking the ENSO (Nino3.4 index) with local climate (rainfall and temperature), rodent population density (capture rate), and human HTNV infections. The multiyear periodicity in winter temperature and annual rainfall may drive *A. agrarius* population fluctuations, as shown in Fig. 2, together with seasonal forcing on the transmission rate in Fig. 4, shaping interannual cycles of climate–animal–HFRS outbreaks.

and zoonotic disease (41), especially the outbreak of hantavirus pulmonary syndrome in the Four Corners region of the United States (22, 24, 42). However, the pathways from global climate to rodent host and the resulting pathogen transmission and spillover through local climate is far from clear (4). In this study, we have shown that ENSO could influence rodent population size and impact interannual cycles of HFRS epidemics. Once the animal dynamics and climate conditions are taken into account, clear evidence emerges for the role that multiyear climate variability plays in the fluctuations of zoonotic diseases. La Niña-related rainfall may increase the capture rate of *A. agrarius* and the risk of HTNV transmission, whereas El Niño-related drought may limit rodent survival and, in turn, reduce the risk of outbreak (Fig. 1*B*). Both El Niño and La Niña events strongly affect zoonotic ecology and have significant implications for public health (43, 44). Locally, drought and positive rainfall anomalies occur during these ENSO years and are associated with epidemic fluctuations.

The fit of the full model accounts for most of the variability in the number of HFRS cases; however, the mechanism of HTNV transmission within the wildlife reservoir is complex (26). In this study, the dynamics of HTNV prevalence in rodents was estimated by the incidence of HFRS and the population density of the rodent. However, the relationship between the intrinsic dynamics and extrinsic drivers of HTNV transmission at the human–animal interface (e.g., the effect of summer climate condition on HFRS outbreaks) requires further research.

In summary, this study lays down the necessary foundation to predict future HFRS epidemics and to develop an early warning system to enhance public health measures, especially in developing countries or areas undergoing social transformation. The real-time monitoring of wildlife dynamics and climate signatures we have outlined above are key in predicting potential HFRS outbreaks.

Materials and Methods

Data Collection and Management. The HFRS dataset consists of monthly clinical cases from 1960 to 2013 in the Wehei Plain of Central China, one of the largest plains in the country (Fig. 1*A*). HFRS cases were confirmed according to standard diagnostic procedures set by the Ministry of Health of the People's Republic of China. Serum samples were sent to the Shaanxi Centre for Disease Control and Prevention (CDC) for the detection of hantavirus-reactive antibodies. Serological and genetic analyses confirmed that all HFRS cases were caused by HTNV (25, 45). In our study, epidemiological data were collected from the Shaanxi Provincial Notifiable Disease Surveillance System.

Surveillance of striped field mice (*A. agrarius*) abundance was conducted in Hu County (108° E, 34° N, an area of 1,255 km^2; shown in Fig. 1*A*) on a monthly basis from 1980 to 2013, by using a standard approach (46). A density-of-rodent population survey was conducted in fields at nine trapping sites where rodents were likely to be present. The study followed a robust design for three consecutive nights each month, where a minimum of 100 traps were set each night and recovered in the morning (at least 300 trap-nights were set each month; the mean number of trap-nights per month was 687, and the SD was 543). Traps were placed outdoors (set as 4 parallel lines of 25 traps each and spaced at 5-m intervals). Rodents were removed from the traps once captured. The capture rate was calculated as the number of *A. agrarius* individuals captured divided by the number of trap-nights.

Since 1960, ~150,000 HFRS cases were reported in the Weihe Plain area. The average annual incidence of HFRS was ~20 cases per 100,000 inhabitants, with the highest incidence (>85 cases per 100,000 inhabitants) occurring in 1984. The population density of striped field mouse (*A. agrarius*), the primary reservoir of HTNV and the dominant species, was monitored and recorded annually from 1980 to 2013. A total of 5,985 *A. agrarius* individuals were captured over 283,620 trap-nights in the field, with a capture rate of 2 individuals per 100 trap-nights.

The daily record of climatic variables, including temperature and rainfall, were obtained from local meteorological stations from 1960 to 2013 (Fig. 1*A*). The ENSO index used in this study is the Nino3.4, which is calculated as the difference between the monthly average sea-surface temperatures for the areas within 5°N, 5°S, 120°W, and 170°W. Time series for the population sizes of inhabitants were obtained from the Shaanxi Statistical Yearbook.

Climate Forcing on Wildlife Reservoir Dynamics. We modeled climate conditions as a general model to describe the observed dynamics with a minimum number of biological assumptions, based on a model proposed by Berryman (47, 48). To measure the environmental forcing related to rodent population dynamics, we created 1,000 populations. The initial (year 1960) capture rate of each artificial population was set as a random value between 0 and 0.1 from a uniform distribution. Each artificial population was then assigned a set of parameter coefficients estimated from a corresponding training subdataset, which contained randomly sampled 80% of the full dataset. We applied the discrete-time model to describe the rodent population fluctuations on an annual scale using the GAMs framework with the mgcv package of R. The use of the GAM framework permits estimation of the unknown function f for each climate variable (49). A total of 1,000 time series of rodent populations were generated by multistep prediction and were compared with the observed capture rates during 1980–2013 to choose the optimal model based on R^2. The model reads:

$$A_{y+\Delta y} = A_y \cdot e \wedge R_y \quad [1]$$

$$R_y = \ln\left(\frac{A_{y+\Delta y}}{A_y}\right) = f_1\left(Rainfall_y\right) + f_2\left(Temperature_y^{winter}\right), \quad [2]$$

where R_y is the population growth rates, and A_y is the capture rate of *A. agrarius* in year *y*. *Temperature* and *Rainfall* represent the temperature in the previous winter and annual rainfall in the previous year, respectively. Δy is the yearly time step of the model, and the function f describes the effect of rainfall or winter temperature on changes in rodent population size.

Structural Equation Model. The structural equation models (SEMs) were implemented to estimate the structural correlation between variables. Yearly and seasonal climate variables were considered to measure the direct and indirect pathways underscoring HFRS epidemics. SEMs were implemented by using the R package lavaan (50) with maximum-likelihood estimation procedures.

Climate Drives Zoonotic Outbreaks. We modeled the dynamics of HTNV spillover into the human population using several potential explanatory variables. HTNV spillover into the human population is considered to be facilitated by the capture rate of *A. agrarius* and climate variables, both representing key drivers of infection. We avoided explicit consideration of the complex mechanism between virus prevalence in rodents and environmental noise by representing HTNV prevalence dynamics in rodents through a model for the force of human infections (number of HFRS cases). A GAM with a Poisson distribution and a log link is used to model the data as:

$$I_{t+1} = (I_t(A_t + \tau))^{\alpha}\beta_t S_t. \quad [3]$$

For the human component, I_t is the number of HFRS cases, and S_t represents the number of individuals susceptible to infection (and hence disease) at time t. The parameter α allows for nonlinearities in contact rates. A_t is the capture rate of *A. agrarius* in month t. β_t is the pathogen transmission rate of hantavirus from rodent to human and is a key parameter that varies over time. The parameter τ represents low, random abundances when no animals were caught. We model this by forcing the rate of change with two extrinsic drivers, namely, seasonality and climate covariates (here temperature and rainfall): $\beta_t = \beta_{seas}\beta_{clim}$. The transmission rate β_t is governed by:

$$\beta_{clim,t} = \delta_1 Rainfall_{t-4} + \delta_2 Rainfall_{t-2} + \delta_3 Temperature_{t-5} + \delta_4 Temperature_{t-4} + \varepsilon \quad [4]$$

$$\beta_{seas,t} = \sum_{i=1}^{n} \varphi_i \Delta_i Month_i \quad [5]$$

$$\log(I_{t+1}) = \alpha\log(I_t) + \alpha\log(A_t + \tau) + \log\left(\beta_{seas,t}\beta_{clim,t}\right) + \log(S_t), \quad [6]$$

where *Temperature* and *Rainfall* are the monthly average temperature and accumulated rainfall, respectively, and time lags are determined by wavelet coherence analyses (*SI Appendix*, Fig. S7). δ is a vector of coefficients for the independent variables. Seasonality is modeled nonparametrically, and φ_i is composed of $n = 12$ distinct values, one for each month. Δ is a vector of dummy variables of length 12. To assess the accuracy of the model, we sampled 70% of the dataset for training runs and used the remaining 30% to test the model. Model fitting and convergence (51) were performed by Metropolis–Hastings Markov chain Monte Carlo algorithm using the MATLAB (Version R2009b) toolbox DRAM (Delayed Rejection Adaptive Metropolis) (52). In model parameterization, the prior distributions for the parameters were Gaussian, with a mean of 0 and a variance of

10^5. We ran the chain for 5 million iterations sampled every 1,000th step after a burn-in of 1 million iterations.

Wavelet. Wavelet analyses were performed to investigate periodicity and coherence of ecological time series (53). In this study, we adopted the Morlet wavelet and beta surrogate significance tests (54, 55). To quantify the time-evolving periodic components of a time series, the wavelet power spectrum was used based on the wavelet transform $W_x(f,t)$ of the time series $x(t)$, which can be regarded as a generalization of the Fourier transform (53, 55).

ACKNOWLEDGMENTS. We thank Sari C. Cunningham for valuable comments and help; and the many hundreds of CDC staff and local health workers in Shaanxi Province who collected data from 1960 to 2013. This work was supported by National Key Research and Development Program of China Grant 2016YFA0600104; National Natural Science Foundation of China Grant 81673234; the health industry's special research funds for public welfare projects (Grant 201502020); Shaanxi Provincial Projects for Serious Disease Prevention and Control Grant 0617-15240415; and Science and Technology Project of Shaanxi Province Grants 2014A7 and 2013K12-04-02.

1. Koelle K, Rodó X, Pascual M, Yunus M, Mostafa G (2005) Refractory periods and climate forcing in cholera dynamics. *Nature* 436:696–700.
2. Cazelles B, Chavez M, McMichael AJ, Hales S (2005) Nonstationary influence of El Niño on the synchronous dengue epidemics in Thailand. *PLoS Med* 2:e106.
3. Laneri K, et al. (2010) Forcing versus feedback: Epidemic malaria and monsoon rains in northwest India. *PLOS Comput Biol* 6:e1000898.
4. Carver S, et al. (2015) Toward a mechanistic understanding of environmentally forced zoonotic disease emergence: Sin Nombre Hantavirus. *Bioscience* 65:651–666.
5. Yu PB, et al. (2015) Hantavirus infection in rodents and haemorrhagic fever with renal syndrome in Shaanxi province, China, 1984-2012. *Epidemiol Infect* 143:405–411.
6. Schmaljohn CS, et al. (1985) Antigenic and genetic properties of viruses linked to hemorrhagic fever with renal syndrome. *Science* 227:1041–1044.
7. Jonsson CB, Figueiredo LTM, Vapalahti O (2010) A global perspective on hantavirus ecology, epidemiology, and disease. *Clin Microbiol Rev* 23:412–441.
8. Schmaljohn C, Hjelle B (1997) Hantaviruses: A global disease problem. *Emerg Infect Dis* 3:95–104.
9. Zhang YZ, Zou Y, Fu ZF, Plyusnin A (2010) Hantavirus infections in humans and animals, China. *Emerg Infect Dis* 16:1195–1203.
10. Lee HW, et al. (1981) Observations on natural and laboratory infection of rodents with the etiologic agent of Korean hemorrhagic fever. *Am J Trop Med Hyg* 30: 477–482.
11. Hutchinson KL, Rollin PE, Peters CJ (1998) Pathogenesis of a North American hantavirus, Black Creek Canal virus, in experimentally infected *Sigmodon hispidus*. *Am J Trop Med Hyg* 59:58–65.
12. Glass GE, Childs JE, Korch GW, LeDuc JW (1988) Association of intraspecific wounding with hantaviral infection in wild rats (*Rattus norvegicus*). *Epidemiol Infect* 101: 459–472.
13. Mills JN, et al. (1997) Patterns of association with host and habitat: Antibody reactive with Sin Nombre virus in small mammals in the major biotic communities of the southwestern United States. *Am J Trop Med Hyg* 56:273–284.
14. Hjelle B, Torres-Pérez F (2010) Hantaviruses in the Americas and their role as emerging pathogens. *Viruses* 2:2559–2586.
15. Mills JN, Yates TL, Ksiazek TG, Peters CJ, Childs JE (1999) Long-term studies of hantavirus reservoir populations in the southwestern United States: Rationale, potential, and methods. *Emerg Infect Dis* 5:95–101.
16. Tian HY, et al. (2015) Changes in rodent abundance and weather conditions potentially drive hemorrhagic fever with renal syndrome outbreaks in Xi'an, China, 2005-2012. *PLoS Negl Trop Dis* 9:e0003530.
17. Zhang WY, et al. (2010) Climate variability and hemorrhagic fever with renal syndrome transmission in Northeastern China. *Environ Health Perspect* 118:915–920.
18. Yan C, et al. (2013) Agricultural irrigation mediates climatic effects and density dependence in population dynamics of Chinese striped hamster in North China Plain. *J Anim Ecol* 82:334–344.
19. Xiao H, et al. (2013) Investigating the effects of food available and climatic variables on the animal host density of hemorrhagic Fever with renal syndrome in Changsha, China. *PLoS One* 8:e61536.
20. Clement J, et al. (2009) Relating increasing hantavirus incidences to the changing climate: The mast connection. *Int J Health Geogr* 8:1.
21. Glass GE, Shields T, Cai B, Yates TL, Parmenter R (2007) Persistently highest risk areas for hantavirus pulmonary syndrome: Potential sites for refugia. *Ecol Appl* 17:129–139.
22. Glass GE, et al. (2000) Using remotely sensed data to identify areas at risk for hantavirus pulmonary syndrome. *Emerg Infect Dis* 6:238–247.
23. Luis AD, Douglass RJ, Mills JN, Bjørnstad ON (2010) The effect of seasonality, density and climate on the population dynamics of Montana deer mice, important reservoir hosts for Sin Nombre hantavirus. *J Anim Ecol* 79:462–470.
24. Glass GE, et al. (2002) Satellite imagery characterizes local animal reservoir populations of Sin Nombre virus in the southwestern United States. *Proc Natl Acad Sci USA* 99:16817–16822.
25. Tian H, et al. (2017) Anthropogenically driven environmental changes shift the ecological dynamics of hemorrhagic fever with renal syndrome. *PLoS Pathog* 13: e1006198.
26. Luis AD, Douglass RJ, Mills JN, Bjørnstad ON (2015) Environmental fluctuations lead to predictability in Sin Nombre hantavirus outbreaks. *Ecology* 96:1691–1701.
27. Samia NI, et al. (2011) Dynamics of the plague-wildlife-human system in Central Asia are controlled by two epidemiological thresholds. *Proc Natl Acad Sci USA* 108: 14527–14532.
28. Thibault KM, Brown JH (2008) Impact of an extreme climatic event on community assembly. *Proc Natl Acad Sci USA* 105:3410–3415.
29. Xiao H, et al. (2013) Atmospheric moisture variability and transmission of hemorrhagic fever with renal syndrome in Changsha City, Mainland China, 1991-2010. *PLoS Negl Trop Dis* 7:e2260.
30. Lloyd-Smith JO, et al. (2009) Epidemic dynamics at the human-animal interface. *Science* 326:1362–1367.
31. Aars J, Ims RA (2002) Intrinsic and climatic determinants of population demography: The winter dynamics of tundra voles. *Ecology* 83:3449–3456.
32. Korslund L, Steen H (2006) Small rodent winter survival: Snow conditions limit access to food resources. *J Anim Ecol* 75:156–166.
33. Korpela K, et al. (2013) Nonlinear effects of climate on boreal rodent dynamics: Mild winters do not negate high-amplitude cycles. *Glob Change Biol* 19:697–710.
34. Yoccoz NG, Stenseth NC, Henttonen H, Prévot-Julliard AC (2001) Effects of food addition on the seasonal density-dependent structure of bank vole *Clethrionomys glareolus* populations. *J Anim Ecol* 70:713–720.
35. Rosenzweig ML, Abramsky Z (1985) Detecting density-dependent habitat selection. *Am Nat* 126:405–417.
36. Scheibler E, Roschlau C, Brodbeck D (2014) Lunar and temperature effects on activity of free-living desert hamsters (*Phodopus roborovskii*, Satunin 1903). *Int J Biometeorol* 58:1769–1778, 10.1007/s00484-00013-00782-00484.
37. Rezende EL, Cortés A, Bacigalupe LD, Nespolo RF, Bozinovic F (2003) Ambient temperature limits above-ground activity of the subterranean rodent *Spalacopus cyanus*. *J Arid Environ* 55:63–74.
38. Hardestam J, et al. (2007) Ex vivo stability of the rodent-borne Hantaan virus in comparison to that of arthropod-borne members of the Bunyaviridae family. *Appl Environ Microbiol* 73:2547–2551.
39. Kallio ER, et al. (2006) Prolonged survival of Puumala hantavirus outside the host: Evidence for indirect transmission via the environment. *J Gen Virol* 87:2127–2134.
40. Stenseth NC, et al. (2002) Ecological effects of climate fluctuations. *Science* 297: 1292–1296.
41. Hjelle B, Glass GE (2000) Outbreak of hantavirus infection in the Four Corners region of the United States in the wake of the 1997-1998 El Nino-Southern Oscillation. *J Infect Dis* 181:1569–1573.
42. Mills JN (2005) Regulation of rodent-borne viruses in the natural host: Implications for human disease. *Arch Virol Suppl* 19:45–57.
43. Kovats RS, Bouma MJ, Hajat S, Worrall E, Haines A (2003) El Niño and health. *Lancet* 362:1481–1489.
44. Engelthaler DM, et al. (1999) Climatic and environmental patterns associated with hantavirus pulmonary syndrome, Four Corners region, United States. *Emerg Infect Dis* 5:87–94.
45. Ma C, et al. (2012) Hantaviruses in rodents and humans, Xi'an, PR China. *J Gen Virol* 93:2227–2236.
46. Ministry of Health (1998) *Handbook of Epidemic Hemorrhagic Fever Prevention and Control* (China People's Health, Beijing).
47. Berryman AA (1992) On choosing models for describing and analyzing ecological time series. *Ecology* 73:694–698.
48. Berryman AA (1999) *Principles of Population Dynamics and Their Application* (Stanley Thornes, Cheltenham, UK).
49. Wood SN (2000) Modelling and smoothing parameter estimation with multiple quadratic penalties. *J R Stat Soc B* 62:413–428.
50. Rosseel Y (2012) lavaan: An R package for structural equation modeling. *J Stat Softw* 48:1–36.
51. Gelman A, Rubin DB (1992) Inference from iterative simulation using multiple sequences. *Stat Sci* 7:457–472.
52. Haario H, Laine M, Mira A, Saksman E (2006) DRAM: Efficient adaptive MCMC. *Stat Comput* 16:339–354.
53. Cazelles B, Chavez M, Magny GC, Guégan J-F, Hales S (2007) Time-dependent spectral analysis of epidemiological time-series with wavelets. *J R Soc Interface* 4:625–636.
54. Rouyer T, Fromentin J-M, Stenseth N, Cazelles B (2008) Analysing multiple time series and extending significance testing in wavelet analysis. *Mar Ecol Prog Ser* 359:11–23.
55. Cazelles B, Cazelles K, Chavez M (2013) Wavelet analysis in ecology and epidemiology: Impact of statistical tests. *J R Soc Interface* 11:20130585.